Probabilistic assessment of port operation downtimes under climate change

P. Camus*

camusp@unican.es

A. Tomás

G. Díaz-Hernández

B. Rodríguez

C. Izaguirre

I.J. Losada

Environmental Hydraulics Institute, Universidad de Cantabria - Avda. Isabel Torres, 15, Parque Científico y Tecnológico de Cantabria, 39011, Santander, Spain

*Corresponding author.

Abstract

Disruptions in harbor operations have significant implications for local, regional and global economies due to ports strategic role as part of the supply chain. A probabilistic evaluation of port operations considering the influence of climate change is required in order to secure optimal exploitation during their useful life. Here, we propose a hybrid statistic-dynamical framework combining a weather generator and a metamodel. The stochastic generator is based on weather types to project climate variability on hourly multivariate dependent climate drivers outside ports. The metamodel efficiently transforms hourly sea conditions from the entrance of the harbor towards the inside port adding the advantages of a physical process model. Thousands of hourly synthetic time series based on present climate conditions and future ones were transferred inside the port to perform a probabilistic analysis of port operations. Future forcing conditions were defined adding several sea level rise (SLR) scenarios, sampled from their probability distribution, to the synthetic sea level fluctuation time series. Wave amplification due to non-linear interactions between wave and sea level variations and changes in the reflection coefficients inside the port induced by SLR were modelled. Probabilistic future changes of operation downtimes were quantified considering the uncertainty associated with the historical forcing conditions outside the port and likely SLR scenarios. The methodology was applied to a specific case study on a regional port located in the north coast of Spain, were port operability due to wave agitation was assessed.

1 Introduction

Port infrastructure is strategic for local, regional and global economic growth and development. They play a crucial role as transportation hubs and gateways for the vast majority of goods transported around the world, linking local and national supply chains to global markets. Moreover, demands on ports are likely to grow in the light of expected increases in world freight volumes, due to shipping efficiency and its smaller carbon footprint compared to other modes of transport (Becker et al., 2012). Other economic activities, including industry, tourism and fisheries, also flourish around seaports. Thus, any significant disruption in the logistics of seaports can have significant economic implications (Chhetri et al., 2014). Service disruptions alone can cause considerable economic losses in the order of billions of dollars and may have important second-order consequences, not only for regional economies and the quality of life of those who depend directly on the port's functionality, but also for the operation of global supply-chains (Becker et al., 2013).

Due to the type of businesses held around them, seaports are located in one of the most vulnerable areas to climate change impacts, i.e. coastal areas susceptible to sea level rise and increased storm intensity and/or mouths of rivers susceptible to flooding (Becker et al., 2012). Despite this, attention to climate-related impacts in ports is relatively recent (McEvoy et al., 2013). The first international benchmark studies consisted of an analysis of the most vulnerable to climate change port cities in 2070 (Nicholls et al., 2008) based on population and asset exposure to water levels defined as one hundred year storm surge, and a worldwide survey sent to Port Authorities to detect sectorial perceptions regarding port risks due to climate change (Becker et al., 2012), respectively.

The first step in the evaluation of climate change impacts on ports involves reviewing all potential impacts and identifying the main marine variables and the databases available where this information is included (Sánchez-

Arcilla et al., 2016). Sea-level rise used to be the only climate-driver considered in the assessment of climate change impacts, as for example, in the methodology proposed to map vulnerability of port assets to sea-level rise relative to their location (Chhetri et al., 2014). Future wave and storm surge conditions are not available from Global Circulation Models (GCMs) for different Representative Concentration Pathway (RCP) scenarios which are the primary tool for investigating the evolution of the climate system over this century. Therefore, a downscaling approach is required to obtain such future projections in order to take them into account when assessing the impact of climate change in ports. The assessment of climate change effects on port operability (wave agitation) has been already explored considering changes in waves using various Regional Circulation Models (RCMs) for an A1B scenario (Sierra et al., 2015), or by adding the effect of sea level rise (SLR) in combination with wave changes for one GCM for RCP8.5 (Sierra et al., 2017). Another example is the simplified approach presented in (Camus et al., 2017) to assess impacts on port operation due to overtopping at the regional scale. This approach consists of a direct statistical weather-typing downscaling of impact indicators (e.g., number of hours per year with overtopping exceeding a certain threshold), integrating changes in storminess including waves, storm surge and sea level rise. One of the advantages of this statistical downscaling method is that it allows quantifying the uncertainty associated to different scenarios and climate models (30 GCMs for 2 RCPs were projected), which is not possible if only one or a limited number of GCMs or RCMs are considered.

Climate drivers for evaluating infrastructure reliability or port operability are defined outside the port, before local nearshore processes such as breaking, diffraction, or reflection have taken place. Each hourly set of multivariate marine conditions at the entrance of the harbor has to be propagated inside the port using a wave model at high spatial resolution. When climate change is assessed to provide useful information for developing effective adaptation strategies, thousands of different combinations of future forcing variables must be simulated to account for the cascading uncertainty associated with the various scenarios and global/regional models (Ranasinghe, 2016). This multi-scale modelling approach is unaffordable computationally. However, a wide variety of metamodels have been proposed to run wave models for large data sets within a reasonable computational time. Metamodels are, in essence, simplified (and hence computationally efficient) representations of computationally intensive models (Gouldby et al., 2014). The traditional approach is to develop a 'look-up table' which involves running the model for a subset of events defined over a regular grid with a coarse resolution to limit the number of simulations. Two approaches with a different degree of complexity can be applied to predict the results for additional events: selecting the result of the most similar design point as representative of the new event (Sierra et al., 2017), or using linear interpolation techniques. More sophisticated methods are developed based on the combination of a selection algorithm and radial basis functions (Camus et al., 2011). This method has been proved to be quite efficient (Gouldby et al., 2017) since it represents the selected input boundary conditions properly and proposes a powerful interpolation technique. Another alternative which doesn't involve numerical simulations consists of applying artificial neural networks to assess port operability (López et al., 2015), but it requires instrumental data outside and inside the port.

To assess the safety, serviceability and exploitation of port operations, Spanish Recommendations for Maritime Structures (ROM 0.0–0.1 (ROM 0.0, 2001),) propose a Level III Verification Method based on Monte Carlo methods for the probabilistic evaluation of failure modes and operational stoppage modes (downtime) of maritime structures. Modes of failure or operability are determined by non-linear interactions of multiple meteo-oceanic dynamics (e.g., astronomical tide, storm surge, waves), climate drivers (waves and storm surge) being statistically dependent due to a common synoptic-scale atmospheric circulation generation. It is therefore necessary to use simulation methodologies that address the dependency among variables. There is a wide range of multivariate statistical models that have been applied to marine conditions. Depending on the type of outputs they provide, models can be divided into two categories: 1) extreme events such as unconditional approaches ((Heffernan and Tawn, 2004), (Gouldby et al., 2014)); copula methods ((Wahl et al., 2012), (Corbella and Stretch, 2013), (Wahl et al., 2016)); weather-type based models (Rueda et al., 2016) and 2) time series using autoregressive models ((Guedes Soares and Cunha, 2000), (Solari et al., 2012a), (Solari and Losada, 2016)). The use of Monte-Carlo methods for probabilistic analyses demands a high computational effort to assess infrastructure failure modes or port operability. The process is even more complex if the probabilistic verification is also performed including climate change projections.

To our knowledge, only one study has evaluated the effect of climate change in port operability caused by wave agitation due to SLR (three values) and wave changes from one GCM. A metamodel based on the 40 simulations of wave propagation inside the port was applied (Sierra et al., 2017). Inoperability time was obtained as the sum of the frequencies of occurrence from the wave sets exceeding a fixed threshold. No assessment of port operation downtimes due to wave agitation has been performed using a Monte-Carlo approach, nor including climate change.

In this work, we propose an integrated methodology for very long-term probabilistic assessments of port operability due to wave agitation, including the potential effects of climate change. Only port operability due to wave agitation was considered in order to simplify the methodology's description, but the method can be easily extended/used for other applications. The probabilistic verification comprises the use of: 1) a stochastic generator which simulates synthetic multivariate forcing conditions at the entrance of the harbor; and 2) a metamodel to transfer these marine conditions inside the port. Synthetic hourly conditions of wave agitation under present and future climate conditions were evaluated to obtain a probabilistic characterization of port operability and to assess changes due to climate change. Probabilistic sea level rise (SLR) scenarios were considered to account for SLR uncertainty in the evaluation of future operation downtimes. The application of the methodology was particularized to a regional fishing port currently experiencing recurrent downtimes.

The paper is organized as follows: section 2 describes the study area used as a pilot case; section 3 presents the databases required for the application of the methodology and section 4 provides extensive details on the overall methodology which combines a weather generator and a metamodel and describes the impact of climate change on port operations. The application of the methodology to the regional port is presented throughout sections 2–4. Finally, section 5 summarizes and concludes the work.

2 Study area

The Port of Candás (43° 35, 3′ N; 5° 45, 5′ W) is located in the region of Asturias (northwest Spain), bordered to the north by the Cantabrian Sea. The current port land area is over $41.150\,\mathrm{m}^2$ with a berthing length of 72 m. The port's main activities are fishing and recreation (see Fig. 1). The water depth in the inner harbor varies between 1 and 3 m (Fig. 2). The main breakwater has a trapezoidal cross-section consisting of an outer layer of 23 ton concrete cubes, a secondary layer with 2–3 tons of gravel, a 50–1000 kg rubble layer and a core. A concrete crown wall lies on top of the rubble mound breakwater with a crest level of 11.50 m. The geometry and materials of the different natural and artificial structures of the port's inner boundaries cause changes in wave reflection along these boundaries at different water levels. For this case study these variations were included in the agitation model by using different reflection coefficients along the berths and docks for the four sea levels considered (see Fig. 2). Specifically, the following reflection coefficients were considered, according to the typology they represent: dissipative beach (Kr = 0.15), reflecting beach (Kr = 0.20), rubble-mound breakwater (Kr = 0.40), cliff (Kr = 0.60) and vertical wharf (Kr = 0.9). For low and mean tide reflection coefficients were kept constant.
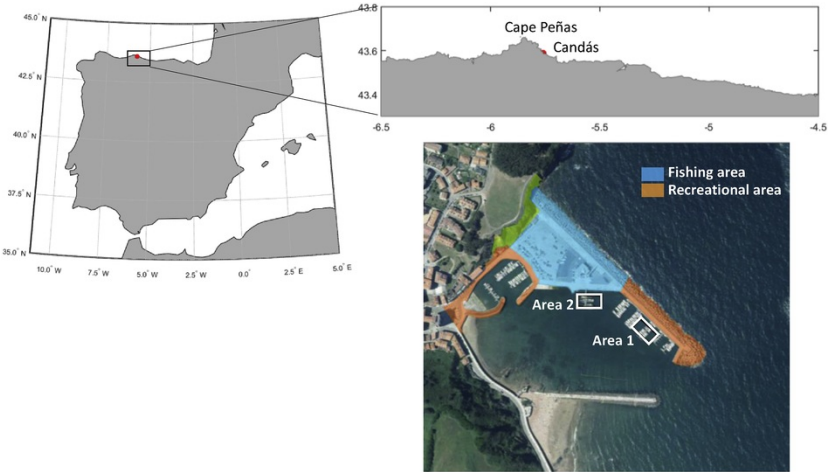

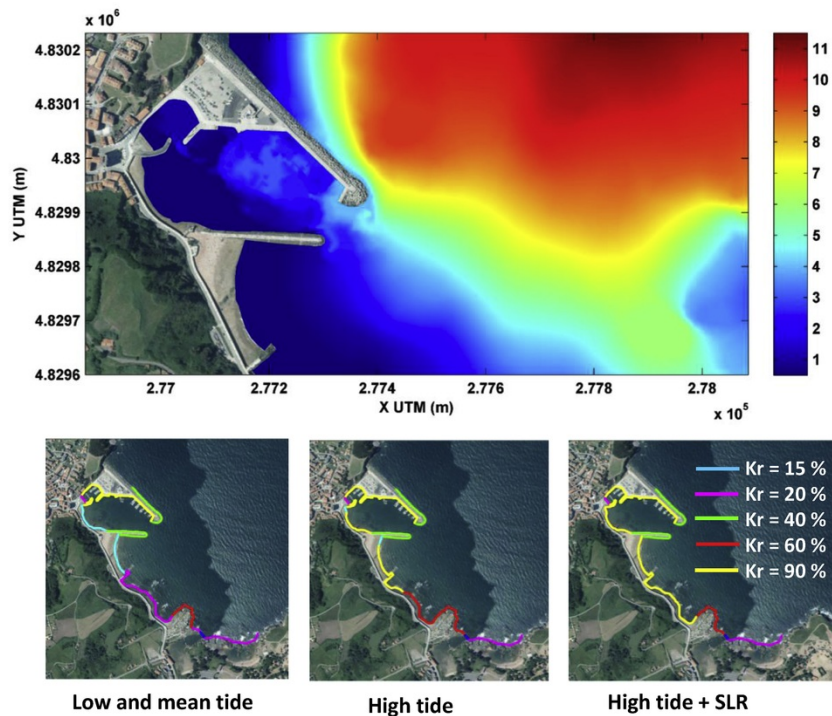**Fig. 1** Location of the Port of Candás in northern Spain.

alt-text: Fig. 1

Fig. 2 Upper figure: Bathymetry of the study area (depth in meters). Lower figures: Reflection coefficients adopted along the port boundaries under different sea levels: low and mean tide, high tide and high tide + SLR. Kr = 0.15 for dissipative beach, Kr = 0.20 for reflecting beach, Kr = 0.40 for rubble-mound breakwater, Kr = 0.60 for cliff and Kr = 0.9 for vertical wharf.

alt-text: Fig. 2

3 Databases

Sea level pressure fields of the Climate Forecast System Reanalysis (CFSR and CFSRv2 (Saha et al., 2014);) were used to define the predictor of the statistical models explained in section 4. The temporal coverage spanned from 1979 to 2013, with an hourly temporal resolution and a 0.5° spatial resolution.

The historical wave information used was the high resolution coastal wave database Downscaled Ocean Waves (DOW (Camus et al., 2013),), with a low resolution mesh of 0.01° × 0.008° and several nested meshes reaching a maximum resolution of 200 m. This database was generated using a hybrid downscaling methodology which combines statistical techniques and dynamical simulations. The Global Ocean Waves database (GOW (Reguero et al., 2012),) was used at the regional scale as wave forcing to generate the coastal wave reanalysis. The SeaWind database, generated by performing a dynamical downscaling of the NCEP/NCAR wind reanalysis at a spatial scale of 30 km (Menendez et al., 2013), was used as wind forcing. The results of this hybrid downscaling provided the following hourly sea state parameters from 1948 to 2014: significant wave height (H_s), mean period (T_m), peak period (T_p) and wave direction (θ).

The 62-year (1948–2014) high-resolution hindcast of the meteorological sea level component (storm surge, *SS*) (GOS 1.1 (Cid et al., 2014);) was used to determine historical storm surge data. The GOS 1.1 database was developed for Southern Europe using the Regional Ocean Model System (ROMS) with a horizontal resolution of 1/8°(~14 km).

The astronomical tide (AT) was reconstructed on an hourly basis at a spatial resolution of 0.25°, using harmonic analyses on the outcomes of the global model of ocean tides (TPXO7.2) that assimilates data from TOPEX/Poseidon missions and tidal gauges for the common period of waves and storm surge.

The regional SLR by 2100 for RCP8.5 scenarios was extracted from global projections of regional mean sea level values obtained by (Slangen et al., 2014) using a dynamical modelling approach that incorporates regional contributions of land ice, groundwater depletion and glacial isostatic adjustment, including gravitational effects due to mass redistribution.

4 Methodology and results

The methodology described in Fig. 3 is composed of two main parts:

- A weather generator to derive hourly multivariate marine conditions outside the port.

- A metamodel to transfer hourly marine conditions outside the port as generated in the previous step to the inner harbor, in order to obtain wave agitation.
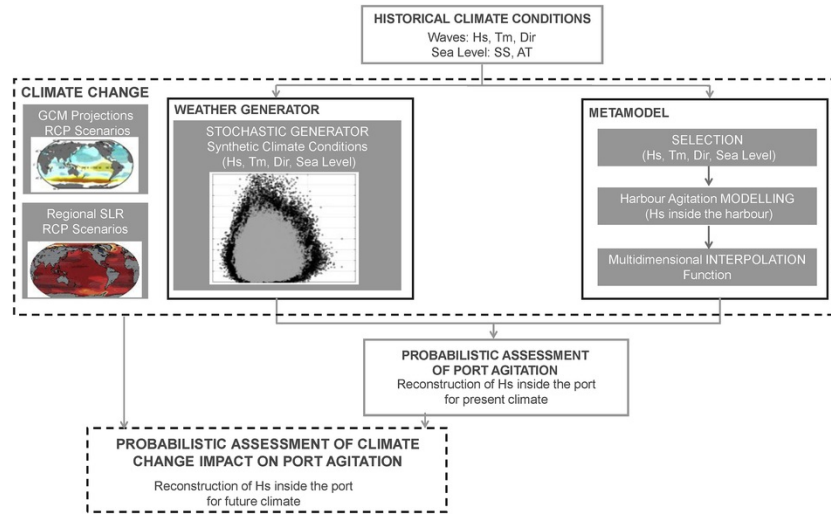

Fig. 3 Probabilistic methodology which combines a weather generator and a metamodel to assess port operability due to wave agitation under present and future conditions.

alt-text: Fig. 3

The definition of the stochastic generator requires historical information of the forcing conditions outside the port. The climate emulator based on weather patterns for modelling daily multivariate events (Rueda et al., 2016) was extended to simulate hourly waves and storm surges at the entrance of the port. The model is based on a predictor-to-predictand synoptic regression-guided classification (Camus et al., 2017), grouping marine conditions according to similar generating meteorological processes, called weather types (WTs). This method ensures that the predictand within each WT is independent and identically distributed for the applicability of Gaussian copulas to model the dependence between variables. Besides, the method captures climate's non-stationary characteristics based on the variability of WTs over time. A Monte Carlo approximation is applied to stochastically simulate large samples of hourly conditions at the entrance of the harbor.

For the second step, a metamodel based on a hybrid downscaling methodology (a combination of dynamical and statistical downscaling) developed to generate high resolution nearshore wave reanalysis databases (Camus et al., 2013) was adopted. Specifically, a number of representative sea states was propagated using a model solving the elliptic mild slope (MSP (GIOC, 2000),) and the time series of nearshore wave parameters) were reconstructed by means of an interpolation technique. The way in which the number of simulations was selected from the synthetic data ensured the coverage of the new multivariate space of climate drivers. The probabilistic assessment of current port operability due to wave agitation was obtained by reconstructing the significant wave height inside the port for each simulated hourly condition at the entrance of the harbor for the present climate.

To assess climate change impacts on port agitation, climate change can be introduced in the weather generator by means of future WT probabilities that can be reflected as changes in waves and storm surges and SLR added to the sea level time series. The metamodel has to be updated to take into account climate change in those cases selected to be modelled as well as the effect of SLR on the reflection coefficients to be used in the wave agitation model.

Fig. 4 shows the time series for years 2013 and 2014 and the distribution of H_s , θ and T_p- θ of the forcing conditions occurring outside the port, obtained from the databases described in section 2. Forcing conditions outside the port were defined at about 6.0 m depth. Wave climate at this location has suffered an intense refraction due to the protection effect of Cape Peñas (Fig. 1) resulting in wave energy concentration in the N-E sector. The maximum significant wave height is limited to 4.5 m while peak periods reach values of 20 s which can be combined with storm surges of almost 0.5 m and high spring tides over 2.0 m.
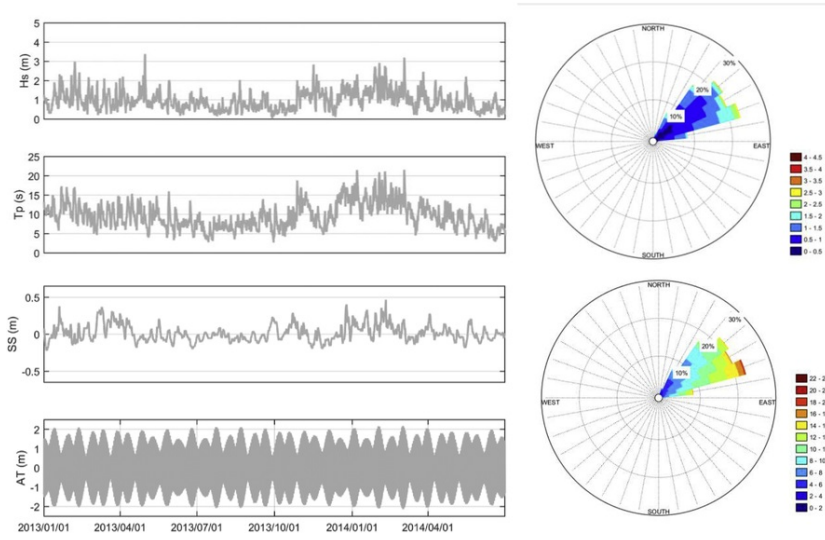
Fig. 4 H_s, T_p, SS and AT values for two years within the time series) at the entrance of the harbor (left panels). H_s and T_p roses (right panels).

alt-text: Fig. 4

4.1 Weather generator

A weather-type framework was used to model the nonstationary behavior of the local multivariate predictand (H_s, T_m, T_p, θ and SS) related with large-scale predictors (sea level pressure, SLP). The daily predictor was classified into a discrete number of weather patterns (WTs) according to their synoptic similarity. Hourly multivariate events were modelled using a marginal distribution for each predictand variable and a Gaussian copula within each WT. The stochastic generator follows similar steps as the one developed by (Rueda et al., 2016) for multivariate extremes, except in this case the extremal index is not required. The five steps involved in this model are: 1) To collect and pre-process historical data of the predictor (SLP) and predictands (H_s, T_m, T_p, θ and SS). 2) Define WTs using a semi-guided classification (Cannon, 2012). 3) Fit a stationary model (e.g. Lognormal, Generalized Extreme Value) to each variable of the multivariate predictand (H_s, T_m, SS outside the port) associated with each WT. 4) Model the dependence between predictand variables within each weather type using a Gaussian copula. 5) Generate synthetic multivariate hourly conditions taking into account the monthly WT probability and dependence structure associated with each WT.

The spatial domain of the predictor should cover the oceanic region responsible for generating waves arriving at each location of interest. The temporal coverage (recent history) should account for wave travel time from generation to target location. Based on previous works, the semi-supervised WTs of the grid node from the global collection of WTs at a 1.0° × 1.0° resolution generated to obtain global wave projections (Camus et al., 2017) at a location closest to the port of study, was used to develop the weather generator (steps 1 and 2 in this section). The predictor definition (spatial domain and temporal coverage) corresponded to the subdomain covering the North Atlantic Ocean (from an ocean division based on a global wave genesis characterization). The predictor was defined as the 3-daily mean SLP and 3-daily mean SLPG (squared SLP gradients), calculated daily throughout the historical time period. More details regarding this characterization and WT collection can be found in (Camus et al., 2017). A regression guided classification was applied to a combination of the weighted predictor and predictand estimations from a regression model linking the SLP fields with local marine conditions. The level of influence of the wave and storm surge data was controlled by a simple weighting factor which balances the loss/gain of predictor/predictand representativeness. A factor equal to 0.6 was implemented based on previous sensitivity analyses. A better grouping of the predictand was obtained due to a stronger relation of the WTs with local marine climate conditions.

The long-term marginal distributions (step 3) of hourly H_s, T_m, and SS outside the port within each WT were fitted to a generalized extreme value (GEV) distribution, a Lognormal distribution or Unified Distribution Model (Solari and Losada, 2012b), obtaining the best fit of the central regime with a GEV. The empirical distribution was used for the wave direction variable. A heteroscedastic model between T_p and T_m was fitted within each WT. Tp was considered to be normally distributed with parameters mean and variance being a function of T_m (polynomials with unknown degree). A Gaussian Copula was used to model the dependence between H_s, T_m, SS and θ (step 4).

The Monte Carlo sampling procedure used to generate synthetic marine conditions (step 5) requires the following phases: i) Sample a daily WT from a Generalized Bernoulli distribution due to the categorical choice of one of the $N = 100$ WTs. ii) Randomly generate 24 hourly synthetic H_s, T_m, θ and SS using the Gaussian copula and the marginal fits associated with the daily simulated WT; iii) Sample 24 hourly T_p from the heteroscedastic model between T_p and T_m associated with the daily WT; iv) Independently sample 24 hourly values of astronomical tide from its monthly empirical distribution. The process is repeated until a synthetic 90-year time series of hourly multivariate forcing

marine conditions is obtained.

One thousand, 90-year long, new time series of H_s, T_m, T_p, θ, SS and AT were simulated with the previously fitted emulator. Each series was generated with a different set of parameters, randomly taken from the parameter sample obtained considering a Gaussian distribution. Scatter plots of the five sea-storm variables are shown in Fig. 5. The large multivariate sample of hourly forcing conditions captures the characteristics of dependencies among variables. Wave breaking and wave steepness limit the maximum simulated wave height. Maximum simulated wave period was limited to 25 s. The effect of the imposed physical limitations of wave slope can be observed in the correct reproduction of the relation between wave heights and small wave periods. Fig. 6 shows the joint probability density functions of (H_s, T_p), (H_s, θ), (H_s, SS) and (T_m, T_p) obtained from the historical series (blue lines) and from the simulated series (dashed lines). The simulated series are able to reproduce the main features of the original bivariate distributions. They fail in representing some details of the distributions, as the clear dependence between wave heights around 1.0 m and low peak periods.
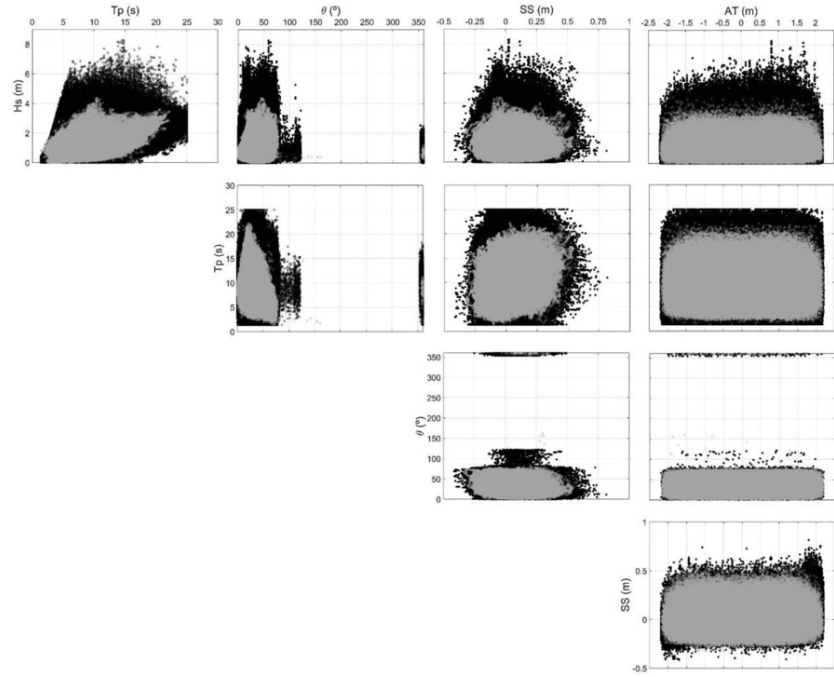

Fig. 5 Scatter plots of marine climate (H_s, T_p, θ, SS, AT) at the entrance of the port. Historical data: grey dots; Monte Carlo simulations (1000 samples of 50 years of hourly data): black dots.
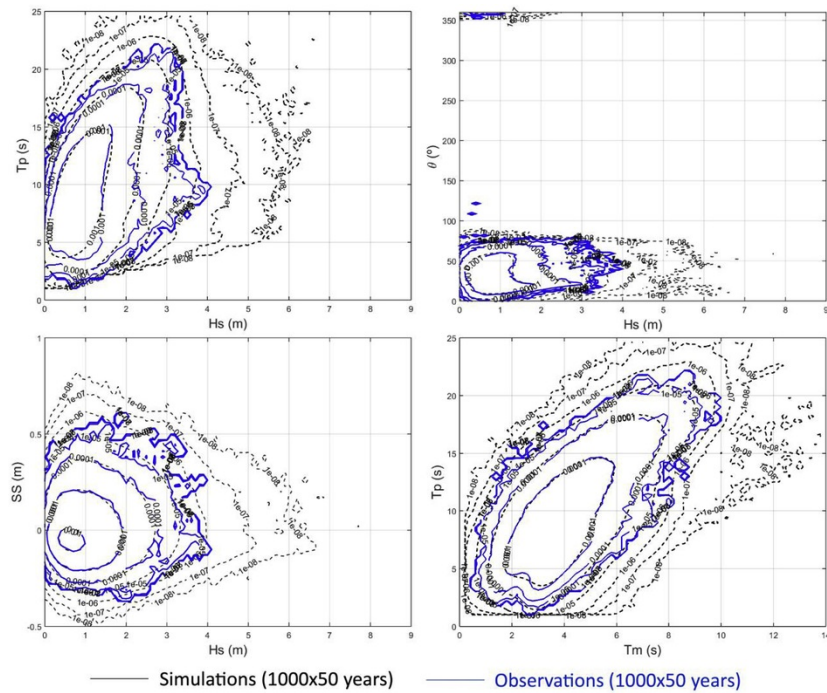
alt-text: Fig. 5

Fig. 6 Joint probability density function of hourly forcing conditions. Blue solid lines represent the results obtained from the historical data and black dashed lines represent the simulated data generated using the weather generator. (For interpretation of the references to color in this figure legend, the reader is referred to the Web version of this article.)

alt-text: Fig. 6

Regarding future synthetic time series (e.g. in the period 2010–2100), climate change can be introduced taking into account changes in storminess by means of future WT probabilities from GCMs and the increase in the mean sea level. Robust multi-model ensemble projections at high spatial resolutions (0.01°x0.008° using DOW at the reference database) measured over the whole century (2010-2099) were estimated along the northern coast of Spain (Toimil et al., 2017). Future wave and storm surge projections were statistically downscaled using a weather-type approach (Camus et al., 2014) for the same 40 GCMs as in regional wave projections made in Europe (Perez et al., 2015). The statistical relationship was established as in the first steps of the weather generator. In this case, however, the empirical probability distribution of each sea state parameter (e.g., significant wave height) associated with each WT was calculated. The distribution of this variable for a certain time period can be estimated as the sum of the probability of each WT during that period multiplied by the corresponding empirical distribution. Different statistics (e.g., mean, 95th percentile) can be derived from the estimated distribution. One of the advantages of this statistical downscaling methodology is that the scale representativeness of the projections depends on the underlying historical wave databases used as a reference (Camus et al., 2017). Fig. 7 shows the multimodel ensemble projections of the annual mean and the 95th percentile of the significant wave height, the mean period and the 95th percentile of storm surge in the area surrounding the port for the period 2070–2099 compared with the 1979-2010 period under the RCP8.5 scenario. Box plots illustrated the uncertainty inherent in future changes obtained from the 40 GCMs. The outcomes reveal slight decreases in surge and wave height and period. These changes are assumed to be negligible compared to the effect of SLR in wave propagation inside the port. Indeed, the decreasing waves and storm surge resulting from these expected changes would underestimate the need for port operation downtimes.
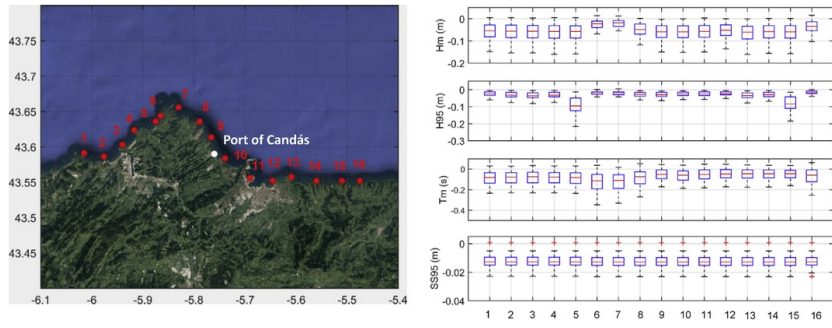
Fig. 7 Regional multimodel projections (RCP8.5, 2070–2099 with respect to 1979–2005) for the mean and the 95th percentile of wave significant wave height, mean wave period and the 95th percentile of storm surge along the coastline surrounding the study port.

alt-text: Fig. 7

Following the approach proposed by (Quinn et al., 2013) to account for the SLR uncertainty in the assessment of flooding risk, a lognormal distribution was fitted with the mean and standard deviation of the regional projections produced by (Slangen et al., 2014) for the RCP8.5 scenarios in 2100 (i.e., 0.63 ± 0.20 m at the study area). The lognormal distribution is considered the most likely distribution representing future SLR (Bamber and Aspinall, 2013), although increased rates of ice sheet loss were not included in this study. The deciles from fitted lognormal distributions split the SLR data set from each horizon year into ten equally probable parts, the 2100 deciles being: 0.377 m; 0.454 m; 0.507 m; 0.553 m; 0.599 m; 0.646 m; 0.699 m; 0.763 m; 0.852 m; and 1.025 m, respectively. Ten curves were derived from local RCP8.5 SLR values in 2025, 2050 and 2100 using a second order polynomial function in order to adopt the shape of those provided by the IPCC (IPCC, 2013Stocker et al., 2013). Hourly SLR time series (2010–2100) derived from these curves were added to the synthetic sea level time series (defined as the sum of storm surge and astronomical tide) to define future forcing conditions of port agitation.

4.2 Metamodel

The steps followed to define the metamodel used to transform all the synthetic forcing conditions outside the port were: 1) selection of a limited number of cases comprising the most representative scenarios of wave and sea level fluctuations (storm-surge, astronomical tide and sea level rise) outside the port; 2) a wave agitation strategy to propagate the selected sea states from the entrance of the bay towards the inner harbor zone; 3) reconstruction of the time series of significant wave heights inside the port.

A subset of sea states ($M = 500$) representative of marine conditions outside the port was selected using the maximum dissimilarity algorithm (MDA (Camus et al., 2011),). The MDA identifies a subset comprising the most dissimilar data in a database. The selection starts by initializing the subset through the transference of one vector from the data sample. The remaining elements are selected iteratively, transferring the most dissimilar one from the remaining data in the database to the subset. Fig. 8 shows the distribution of the selected subset from the MDA over the full multivariate parameter space (H_s, T_p, θ and sea level) covered by the Monte Carlo realizations. The multivariate subset is distributed evenly across the space covering the potential combinations between the four variables with some points selected in the outline of the data space, contributing to an accurate reconstruction of wave agitation conditions inside the port using the proposed metamodel.
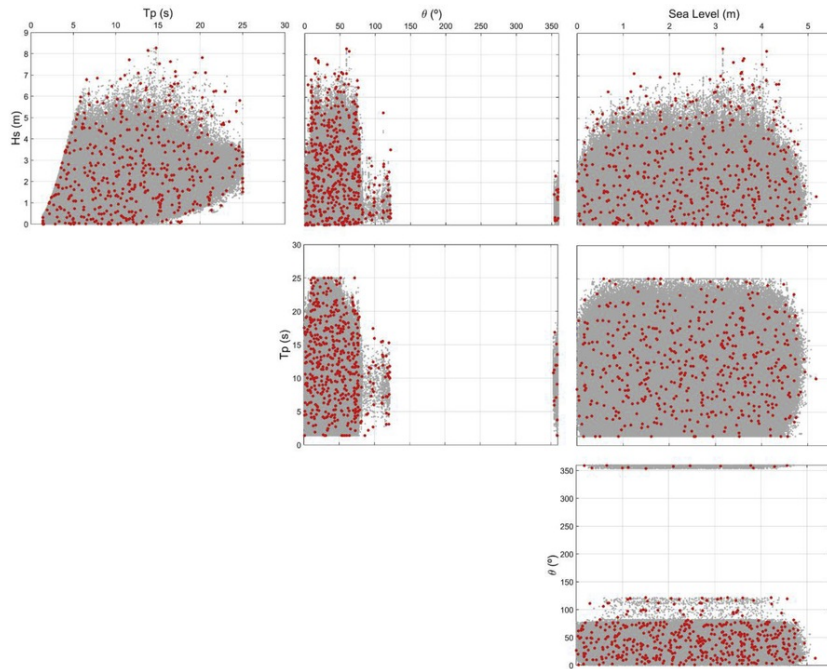
Fig. 8 Scatter plots of simulated data (grey dots) and the selected cases using the MDA (red dots in). (For interpretation of the references to color in this figure legend, the reader is referred to the Web version of this article.)

alt-text: Fig. 8

The MSP numerical model (GIOC, 2000) was used for wave agitation simulations. This model is able to solvewave propagation towards and into the harbor, taking into account the refraction, diffraction, wave breaking and partial reflection imposed by natural and artificial structures (quays, basins, breakwaters, etc.) and real bathymetry contours. The model provides (2DH) significant wave maps along the whole numerical domain. A complete spectral sea-state propagation strategy (Diaz-Hernandez et al., 2015) based on the invocation of a pre-calculated monochromatic wave catalogue was applied to noticeably reduce the CPU-effort to propagate real wave spectra towards any inner control point. This technique is based on a three-step method:

1. The selection of N monochromatic wave conditions (the combination of periods T and directions θ) by collapsing the 4D-hypermatrix [frequency, direction, energy, time] for the whole wave hindcast used, into a single resulting matrix representing the historical energy packs available in the study zone (for a typical 35 frequency x 72 direction spectrum matrix, and taking into account real/theoretical frequency and direction spreading factors for each hour). N can adopt values from 30% to 60% of the total matrix size used, depending on the geographical location of the harbor/outer wave climate.

2. The numerical propagation of each N monochromatic wave (using a constant wave height H, because of the linear nature of the model used) and for the different sea levels considered.

3. The aggregation of any spectrum by adding all the individual energy packs that define it.

For this study additional considerations were established:

4. Four water levels were used (total Nx4 monochromatic cases) (three to cover the astronomical tide range and one as expected upper SLR).

5. Changes in reflection coefficients in the model's setup (as described in the study area section) due to SLR.

This technique, besides achieving a radical CPU-time reduction, enables to rapidly include any future scenario needed or sensitivity analysis required, as well as changes in one or many spectrum variables due to climate change (energy, frequency, direction and its frequency-directional spreading). On the other hand, this technique could over-predict wave-shoaling effects, especially for shallow bathymetry zones. Thus, it should be used with caution if

non-linear wave-wave interactions are expected in the study zone, especially for wave breaking related processes and shoaling. This drawback is minimized for open harbors, with (in general) quasi-constant/mild bathymetry configurations within the basins and outer zones, as shown in (Diaz-Hernandez et al., 2015). Fig. 9 shows an example of a wave agitation map inside the port for conditions outside the port defined by $H_s = 7.2$ m; $T_p = 15.8$ s; $\theta = 54.5°$ and sea level = 3.63 m.

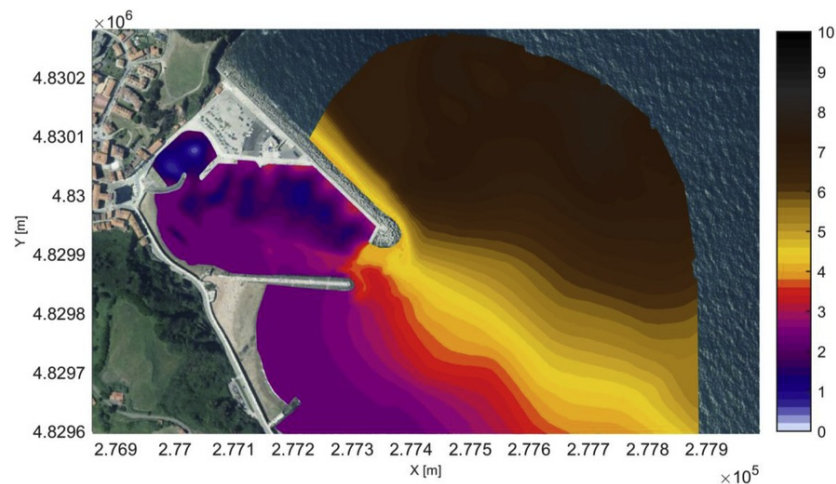**Fig. 9** Wave agitation map for the following marine conditions outside the port: $H_s = 7.2$ m; $T_p = 15.8$ s; $\theta = 54.5°$ and sea level = 3.63 m.

alt-text: Fig. 9

The significant wave height time series inside the port are reconstructed using the multidimensional interpolation technique of radial basis functions (RBF (Rippa, 1999),). The RBFs enable a statistical relationship to be defined between the marine parameters characterizing the forcing conditions and the wave height inside the port from the results of the selected cases. The RBF interpolation method defines the function to be approximated by means of a weighted sum of radially symmetric basic functions located at the data points where the results are available. A more detailed description of these statistical tools implemented in the proposed hybrid methodology can be found in (Camus et al., 2011).

4.3 Results

The synthetic historical time series of marine conditions (waves, storm surge, and astronomical tide) outside the port were transferred inside the port using the corresponding RBF. The synthetic time series outside the port was transformed to the future period 2010–2099 adding the corresponding SLR to each hourly sea level. Their corresponding wave height inside the port was reconstructed applying the RBF.

The annual operability or the hours of non-operability are some of the basic port design criteria stipulated by national and/or international standards (such as ROM or PIANC). In this example, hours of non-operability were calculated from each time series as the hours exceeding a certain threshold of H_s inside the port. Here, a threshold of 0.4 m was applied, as suggested in the Spanish Recommendations for Maritime Structures for Fishing Ports (ROM 3.1–99 (ROM 3.1, 1999),).

Fig. 10 shows the historical and future empirical cumulative distributions of significant wave height, Hs, inside the port in Areas 1 and 2 from the one thousand synthetic time series. Fifty-year long time series of forcing conditions were considered in the assessment of the port's downtimes since the useful life of the Port of Candás is established in 50 years. The future distribution was based on the thousand synthetic future hourly time series from 2050 to 2099 obtained for the ten SLR scenarios sampled from a lognormal distribution of the RCP8.5 SLR projections. The future empirical distributions for the ten SLR scenarios were represented in a yellow-red scale corresponding to the lowest-highest decile, respectively. The probability of a significant wave height lower than 0.4 m (non-operability threshold for fishing ports) is lower the higher the SLR (see the zoomed image of the empirical cumulative distribution between 0.35 and 0.45 m in Fig. 10).
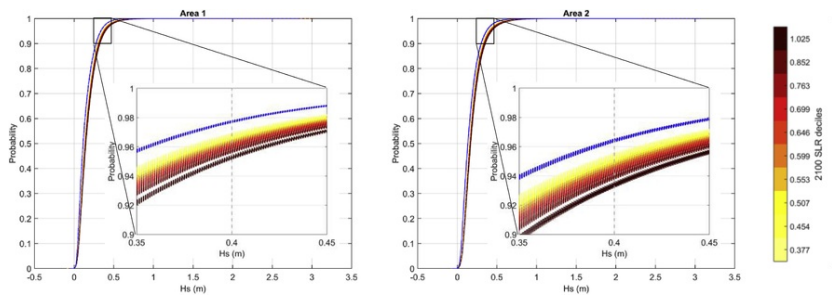
Fig. 10 Historical empirical cumulative distribution (in blue) and future empirical cumulative distributions for the ten SLR scenarios (in yellow-red scale) of significant wave height inside the port in Area 1 and Area 2. (For interpretation of the references to color in this figure legend, the reader is referred to the Web version of this article.)

alt-text: Fig. 10

Hours of non-operability were calculated from the probability (p) obtained for a threshold of 0.4 m as $(1-p) \times 365 \times 24$. The probabilistic distributions of non-operability hours at present (blue) and future (2050–2099, in red) climate conditions are shown in Fig. 11. Future distributions of non-operability for each RCP8.5 SLR scenario are displayed (dashed lines in the yellow-red color scale) with the ensemble mean future probabilistic distribution of non-operability (in red). The ensemble mean distribution was obtained by adding up the distribution for each of the ten SLR scenarios multiplied by 0.1 (the ten SLR scenarios are sampled with an equal probability). It can be noted that hours of non-operability do increase from present to future conditions for both areas.
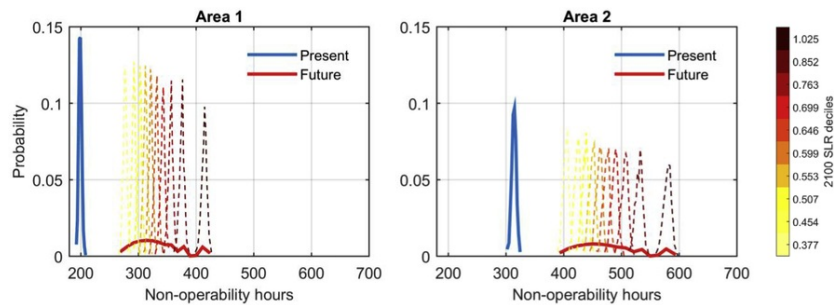

Fig. 11 Probabilistic distributions of non-operability hours due to wave agitation in Areas 1 and 2 inside the port in current (in blue) and future (2050–2099) climate conditions in each SLR scenario (in yellow-red scale) and the future ensemble mean distribution of non-operability hours (thick red line). (For interpretation of the references to color in this figure legend, the reader is referred to the Web version of this article.)

alt-text: Fig. 11

The probabilistic distribution of non-operability hours under current climate conditions represents the uncertainty associated with the historical forcing conditions outside the port. The ensemble mean future distribution integrates the uncertainty associated with the RCP8.5 SLR scenarios and the uncertainty due to the forcing conditions outside the port (distributions of non-operability hours of ten future RCP8.5 SLR scenarios). Besides, higher non-operability hours, as well as a higher uncertainty, are expected for higher SLR scenarios, as can be observed in wider probabilistic distributions of non-operability hours the higher the SLR decile (see Fig. 11).

One additional way to summarize and compare the results obtained is displayed in Table 1. Each of the present and future distributions of non-operability hours is fitted to a lognormal distribution. The mean, standard deviation and coefficient of variation are calculated and shown in the table. In both Areas 1 and 2, the future mean values for non-operability hours are drastically increased (from 198.90 to 332.13 in Area 1 and from 313.62 to 475.14 in Area 2) due to a mean SLR of 0.257 m by 2050 and 0.634 m by 2100. The latter increase is due to non-linear interactions between waves and sea level, and changes in the reflection coefficients associated to SLR. Regarding the nondimensional coefficient of variation, the uncertainty associated with non-operability hours increases from about 1.3% (0.0132 in Area 1 and 0.0129 in Area 2) under current conditions, to around 10% (0.1163 in Area 1 and 0.1044 in Area 2) in future ones. These results differ from the future SLR coefficient of variation (26.7% by 2050 and 31.1% by 2100), indicating that the magnitude of the SLR uncertainties are reflected to a lower degree in the magnitude of the uncertainty of non-operability hours.

Table 1 Mean, Standard Deviation and Coefficient of Variation of the lognormal distribution of 2050 SLR and 2100 SLR predictions and the lognormal distribution of the non-operability hours for the present and

future period in Areas 1 and 2.

alt-text: Table 1

	RCP8.5 SLR (m)		Non-operability (hours)				
			Area 1			Area 2	
	2050	2100	Present	Future (2050–2100)		Present	Future (2050–2100)
Mean	0.257	0.634	198.90	332.13		313.62	475.14
Std	0.069	0.197	2.625	38.61		4.057	49.604
CV (std/mean)	0.267	0.311	0.0132	0.1163		0.0129	0.1044

Non-operability hours during the useful life of the infrastructure/port taking into account climate change was calculated along the 21st century adding the evolution of the SLR to the hourly time series of sea level. In the previous analysis of the impact of climate change in the port's operability, future non-operability hours were calculated for a useful life of 50 years, from 2050 to 2100, to obtain more significant changes. However, the assessment of port operability should be adjusted to the projected useful life of the infrastructure, as of its construction. Fig. 12 shows the interannual variability of the ensemble's mean probability of non-operability hours from 2010 to 2099 in Areas 1 and 2 based on the ten SLR scenarios. First, the empirical distribution of non-operability hours was calculated on a yearly basis for each of the 10 RCP8.5 SLR scenarios considered. Mean sea level rise rates were determined fitting a second order polynomial to the deciles from the local SLR lognormal distribution in 2025, 2050 and 2100. Afterwards, the ensemble mean distribution of non-operability hours was calculated every year. An average moving mean of ten years was applied. A linear trend of the mean hours of non-operability along the 21st century can be observed in Fig. 12 (e.g., downtime increases from 320 h in 2010 to 510 h in 2100). The dispersion of the empirical density distribution rises along the 21st century due to a broader uncertainty of the SLR scenarios as the horizon increases. At the beginning of the 21st century, the SLR distribution spread was limited which is reflected in a narrow ensemble mean distribution of non-operability hours (i.e., high probability centered in the mean value). However, the SLR distribution broadened along the 21st century, increasing the ensemble mean distribution of hours of non-operability (e.g, downtime hours vary from 290 to 400 h in 2010 and from around 400 to 800 in 2100). Changes in non-operability hour values are more significant after 2050 due to a more pronounced acceleration of SLR as of the second half of the 21st century.
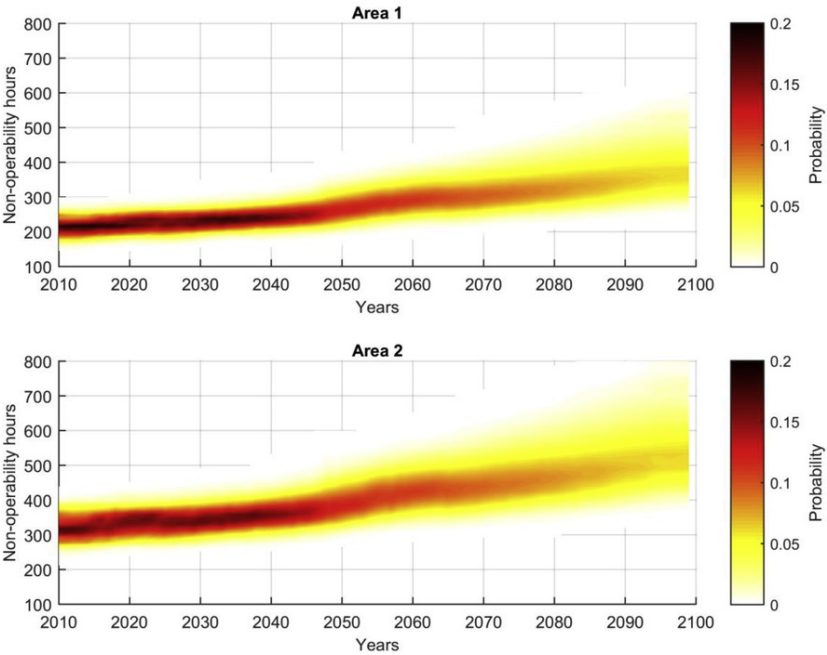
Fig. 12 Interannual ensemble mean probability of non-operability hours from 2010 to 2099 in Area 1 and Area2 taking into account the increase in SLR uncertainty along the 21st century.

alt-text: Fig. 12

5 Summary and conclusions

A hybrid statistical-dynamical framework was developed with two main purposes: 1) to provide a probabilistic evaluation of port operability to assess a minimum level of downtime of the port; 2) to introduce climate change in the assessment of port operability during its useful life.

The methodology is strongly dependent on the multivariate nature of climate drivers of wave agitation such as the combination of waves and sea levels and the availability of these forcings outside the port. Therefore, the following requirements should be met: 1) the use of a stochastic generator to model the dependence between multivariate conditions; 2) the application of a numerical modelling approach to propagate wave offshore conditions inside the port.

Hence, the methodology includes: 1) A weather generator based on WTs to take into account future climate variability through WT probability changes linked to changes in climate drivers (waves and storm surges); 2) A metamodel based on a catalog of wave propagations and a multidimensional non-linear interpolation to reconstruct hourly significant wave height time series inside the port with an accuracy similar to that of the numerical simulations.

The case study was focused on port operability due to wave agitation. The methodology allows to transfer thousands of synthetic time series of present and future climate conditions inside the port in order to carry out a probabilistic analysis of port operability. Future changes in non-operability are expressed including both uncertainties associated with marine conditions outside the port and SLR. Climate induced changes in waves and storm surge are considered to be negligible due to the projections obtained in the study area. Uncertainty of forcing conditions outside the port was quantified through the use of a weather generator that allows to generate synthetic time series. SLR uncertainty was introduced equally by sampling its probability distribution in several horizons, while hourly SLR time series were added to the synthetic sea level fluctuations to define the future forcing conditions outside the port. SLR uncertainty was integrated in the future non-operability evaluation joining the contribution of each sampled SLR scenario with its corresponding probability.

Obtaining the future distribution of non-operability hours allows calculating the future probability associated with the non-operability exceedance hours threshold established in port design recommendations (i.e. ROM 3.1–99 (ROM 3.1, 1999),) during their useful life. The proposed hybrid methodology produces this very useful and relevant outcome to define a specific acceptable operability risk and can be used as a design criterion in new coastal infrastructure or for climate change adaptation plans.

Although for this specific pilot case, climate induced changes on waves and storm surges, have been neglected due to their small values, non-linear feedbacks induced by SLR that may produce an amplification of wave conditions in shallow waters (Arns et al., 2017) have been introduced in the wave agitation model. Future hourly sea conditions are transformed from the harbor's entrance to inside the port considering the non-linearities between tides, surges, waves and SLR. Changes in the reflection coefficient inside the port due to changes in sea level have also been implemented in the wave agitation simulation.

The proposed methodology presents several limitations. The synthetic marine conditions are generated without modelling time structure dependence, which would allow performing an analysis of non-operability's persistence. Besides, this version of the climate emulator is not useful for the analysis of extreme conditions. Synthetic extreme events are not time independent and their frequency could be overestimated. Nevertheless, our objective was focused on port operability which should not be conditioned by extreme events.

The methodology presented can be extended to further applications such as coastal infrastructure reliability or operability for other functional parameters or marine operations by tailoring the weather generator and selecting the most appropriate numerical model.

Acknowledgments

Appendix A. Supplementary data

Supplementary data to this article can be found online at https://doi.org/10.1016/j.coastaleng.2019.01.007.

References

Arns A., Dangendorf S., Jensen J., Talke S., Bender J. and Pattiaratchi C., Sea-level rise induced amplification of coastal protection design heights, *Sci. Rep.* **7**, 2017, 40171 https://doi.org/10.1038/srep40171.

Bamber J.L. and Aspinall W.P., An expert judgement assessment of future sea level rise from the ice sheets, *Nat. Clim. Change* **3**, 2013, 424–427, https://doi.org/10.1038/nclimate1778.

Becker A., Inoue S., Fischer M. and Schwegler B., Climate change impacts on international seaports: knowledge, perceptions, and planning efforts among port administrators, *Climatic Change* **110** (1–2), 2012, 5–29.

Becker A.H., Acciaro M., Asariotis R., Cabrera E., Cretegny L., Crist P., Esteban M., Mather A., Messner S., Naruse S., Ng A.K.Y., Rahmstorf S., Savonis M., Song D.-W., Stenek V. and Velegrakis A.F., A note on climate change adaptation for seaports: a challenge for global ports, a challenge for global society, *Climatic Change* **120** (4), 2013, 683–695.

Camus P., Mendez F.J. and Medina R., A hybrid efficient method to downscale wave climate to coastal areas, *Coast Eng.* **58** (9), 2011, 851–862.

Camus P., Méndez F.J., Medina R., Tomás A. and Izaguirre C., High resolution downscaled ocean waves (DOW) reanalysis in coastal areas, *Coast Eng.* **72**, 2013, 56–68.

Camus P., Menéndez M., Méndez F.J., Izaguirre C., Espejo A., Cánovas V., Pérez J., Rueda A., Losada I.J. and Medina R., A weather-type statistical downscaling framework for ocean wave climate, *J. Geophys. Res.* 2014, https://doi.org/10.1002/2014JC010141.

Camus P., Losada I.J., Izaguirre C., Espejo A., Menéndez M. and Pérez J., Statistical wave climate projections for coastal impact assessments, *Earth's Future* **5** (9), 2017, 918–933.

Cannon A.J., Regression-guided clustering: a semisupervised method for circulation-to-environment synoptic classification, *J. Appl. Meteorol. Climatol.* **51**, 2012, 185–190 https://doi.org/10.1175/jamc-d-11-0155.1.

Chhetri P., Corcoran J., Gekara V., Maddox C. and McEvoy D., Seaport resilience to climate change: mapping vulnerability to sea-level rise, *Spatial Sci.* 2014, https://doi.org/10.1080/14498596.2014.943311.

Cid A., Castanedo S., Abascal A.J., Menéndez M. and Medina R., A high resolution hindcast of the meteorological sea level component for Southern Europe: the GOS dataset, *Clim. Dynam.* 2014, https://doi.org/10.1007/s00382-013-2041-0.

Corbella S. and Stretch D.D., Simulating a multivariate sea storm using Archimedean copulas, *Coast Eng.* **76**, 2013, 68–78.

Diaz-Hernandez G., Mendez F.J., Losada I.J., Camus P. and Medina R., A nearshore long-term infragravity wave analysis for open harbours, *Coast Eng.* **97**, 2015, 78–90.

GIOC, MSP: A Finite Element Model for Wave Agitation in Ports. Technical Report and User Manual, 2000, Universidad de Cantabria, (in Spanish).

Gouldby B., Méndez F.J., Guanche Y., Rueda A. and Mínguez R., A methodology for deriving extreme nearshore sea conditions for structural design and flood risk analysis, *Coast Eng.* **88**, 2014, 15–26.

Gouldby B., Wyncoll D., Panzeri M., Franklin M., Hunt T., Hames D., Tozer N., Hawkes P., Dornbusch U. and Pullen T., Multivariate extreme value modelling of sea conditions around the coast of England, *Proc. Inst. Civ. Eng.: Maritime Eng.* **170** (1), 2017, 3–20.

Guedes Soares C. and Cunha C., Bivariate autoregressive models for the time series of significant wave height and mean period, *Coast Eng.* **40**, 2000, 297–311.

Heffernan J.E. and Tawn J.A., A conditional approach for multivariate extreme values (with discussion), *J. Roy. Stat. Soc.* **66** (3), 2004, 497–546.

IPCC 2013. Climate Change 2013: the Physical Science Basis. Contribution of Working Group I to the Fifth Assessment Report of the Intergovernmental Panel on Climate Change [Stocker, T.F., D. Qin, G.-K. Plattner, M. Tignor, S.K. Allen, J. Boschung, A. Nauels, Y. Xia, V. Bex and P.M. Midgley (eds.)].

López I., López M. and Iglesias G., Artificial neural networks applied to port operability assessment, *Ocean Eng.* **109**, 2015, 298–308.

McEvoy D., Mullett J., Millin S., Scott H. and Trundle A., Understanding Future Risks to Ports in Australia. Work Package 1 of Enhancing the Resilience of Seaports to a Changing Climate Report Series, National Climate Change Adaptation Research Facility, Gold Coast, 2013, 77.

Menendez M., García-Díez M., Fita L., Fernández J., Méndez F.J. and Gutiérrez J.M., High- resolution sea wind hindcasts over the Mediterranean area, *Clim. Dynam.* 2013, https://doi.org/10.1007/s00382-013-1912-8.

Nicholls R.J., Hanson S., Herweijer C., Patmore N., Hallegatte S., Corfee-Morlot J., Chateau J. and Wood R.M., Ranking Port Cities with High Exposure and Vulnerability to Climate Extremes: Exposure Estimates. Environment Working Papers no.1, 2008, OECD.

Perez J., Menendez M., Camus P., Mendez F.J. and Losada I.J., Statistical multi-model climate projections of surface ocean waves in Europe, *Ocean Model.* **96**, 2015, 161–170.

Quinn N., Bates P.D. and Siddall M., The contribution to future flood risk in the Severn Estuary from extreme sea level rise due to ice sheet mass loss, *J. Geophys. Res. Oceans* **118**, 2013, 5887–5898, https://doi.org/10.1002/jgrc.20412.

Ranasinghe R., Assessing climate change impacts on open sandy coasts: a review, *Earth Sci. Rev.* **160**, 2016, 320–332.

Reguero B.G., Menéndez M., Méndez F.J., Mínguez R. and Losada I.J., *A Global Ocean Wave (GOW) Calibrated Reanalysis from 1948 Onwards Coastal Engineering* **vol. 65**, 2012, 38–55.

Rippa S., An algorithm for selecting a good value for the parameter c in radial basis function interpolation, *Adv. Comp. Math.* **11**, 1999, 193–210.

ROM 0.0, General Procedure & Requirements for Design of Maritime & Harbour Structures (Part I); Puertos del Estado, 2001, ISBN: 84-88975-31-7. www.puertos.es.

ROM 3.1, Maritime Port Configuration Design: Approach channel & Harbour basin; Puertos del Estado, 1999, ISBN: 84-88975-52-X. www.puertos.es.

Rueda A., Camus P., Tomás A., Vitousek S. and Méndez F.J., A multivariate extreme wave and storm surge climate emulator based on weather patterns, *Ocean Model.* **104**, 2016, 242–251.

Saha S., Moorthi S., Wu X., Wang J., Nadiga S., Tripp P., Behringer D., Hou Y.T., Chuang H.Y., Iredell M., Ek M., Meng J., Yang R., Mendez M.P.n., van den Dool H., Zhang Q., Wang M. Chen and Becker E., The NCEP climate Forecast system version 2, *J. Clim.* **27**, 2014, 2185–2208, https://doi.org/10.1175/JCLI-D-12-00823.1.

Sánchez-Arcilla A., Sierra J.P., Brown S., Casas-Prat M., Nicholls R.J., Lionello P. and Conte D., A review of potential physical impacts on harbours in the Mediterranean Sea under climate change, *Reg. Environ. Change* **16** (8), 2016, 2471–2484.

Sierra J.P., Casas-Prat M., Virgili M., Mösso C. and Sánchez-Arcilla A., Impacts on wave-driven harbour agitation due to climate change in Catalan ports, *Nat. Hazards Earth Syst. Sci.* **15** (8), 2015, 1695–1709.

Sierra J.P., Genius A., Lionello P., Mestres M., Mösso C. and Marzo L., Modelling the impact of climate change on harbour operability: the Barcelona port case study, *Ocean Eng.* **141**, 2017, 64–78.

Slangen A.B.A., Carson M. and Katsman C.A., Modelling twenty-first century regional sea-level changes, *Climatic Change* 2014, https://doi.org/10.1007/s10584-014-1080-9.

Solari S. and Losada M.A., Unified distribution models for met-ocean variables: application to series of significant wave height, *Coast Eng.* **68**, 2012a, 67–77.

Solari S. and Losada M.T., Simulation of non-stationary wind speed and direction time series, *J. Wind Eng. Ind. Aerod.* **149**, 2016, 48–58.

Solari S. and van Gelder P.H., On the use of vector autoregressive VAR and regime switching VAR models for the simulation of sea and wind state parameters, In: Guedes Soares Carlos, et al., (Eds.), *Marine Technology and Engineering,* 2012b, Taylor & Francis Group; London, 217–230.

Toimil A., Losada I.J., Camus P. and Díaz-Simal P., Managing coastal erosion under climate change at the regional scale, *Coast Eng.* **128**, 2017, 106–122.

Wahl T., Mudersbach C. and Jensen J., Assessing the hydrodynamic boundary conditions for risk analyses in coastal areas: a multivariate statistical approach based on Copula functions, *Nat. Hazards Earth Syst. Sci.* **12** (2), 2012, 495–510.

Wahl T., Plant N.G. and Long J.W., Probabilistic assessment of erosion and flooding risk in the northern Gulf of Mexico, *J. Geophys. Res. Oceans* **121**, 2016, https://doi.org/10.1002/2015JC011482.

Appendix A. Supplementary data

The following is the supplementary data to this article:

Multimedia Component 1

Data Profile

alt-text: Data Profile

Highlights

- Probabilistic evaluation of climate change impacts on port operations taking into account the uncertainty due to SLR projections.

- A hybrid statistical-dynamical framework is proposed for probabilistic assessment of port agitation but can be applied to define design criteria with an specific acceptable operability risk or for climate change adaptation plans.

- The framework combines a weather generator to introduce the uncertainty of multivariate marine forcing conditions and a metamodel for an efficient numerical modelling.

Queries and Answers

Query: Highlights should only consist of "125" characters per bullet point, including spaces. The highlights provided are too long; please edit them to meet the requirement.

Answer: · Probabilistic evaluation of climate change impacts on port operations including the uncertainty due to SLR projections.

· The proposed hybrid framework combines a weather generator and a metamodel for an efficient physical-process modelling

· The framework can be applied to define design criteria with an specific acceptable operability risk.

· The framework can be used for climate change adaptation plans.

Query: Please confirm that the provided email "camusp@unican.es" is the correct address for official communication, else provide an alternate e-mail address to replace the existing one, because private e-mail addresses should not be used in articles as the address for communication.

Answer: Yes, it is correct

Query: Solari and Losada, 2012b cited in the text and list has been changed to Solari and Losada, 2012 because there is only one Solari and Losada, 2012 in the article. Please check, and correct if necessary.

Answer: Ok, it is correct as you propose. There are two references of Solari in 2012 but with different co-autor. Solari S. and Losada M.A, 2012   Solari S. and van Gelder P.H., 2012

Query: Have we correctly interpreted the following funding source(s) and country names you cited in your article: European Regional Development Fund, European Union; Spanish 'Ministerio de Economía y Competitividad' (MINECO)?

Answer: Yes

Query: Please confirm that given names and surnames have been identified correctly and are presented in the desired order and please carefully verify the spelling of all authors' names.

Answer: Yes

Query: Your article is registered as a regular item and is being processed for inclusion in a regular issue of the journal. If this is NOT correct and your article belongs to a Special Issue/Collection please contact s.natarajan.2@elsevier.com immediately prior to returning your corrections.

Answer: Yes